

# Flux flow of Abrikosov-Josephson vortices along grain boundaries in high-temperature superconductors

A. Gurevich<sup>1</sup>, M.S. Rzchowski<sup>1,2</sup>, G. Daniels<sup>1</sup>, S. Patnaik<sup>1</sup>,

B.M. Hinaus<sup>3</sup>, F. Carillo<sup>4</sup>, F. Tafuri<sup>4</sup>, and D.C. Larbalestier<sup>1</sup>.

<sup>1</sup>*Applied Superconductivity Center, University of Wisconsin, Madison, Wisconsin*

<sup>2</sup>*Department of Physics, University of Wisconsin, Madison, Wisconsin*

<sup>3</sup>*Department of Physics, University of Wisconsin, Stevens Point, Wisconsin and*

<sup>4</sup>*Universita di Napoli Federico II, Dipartimento di Scienze Fisiche, Italy*

(Dated: October 25, 2018)

We show that low-angle grain boundaries (GB) in high-temperature superconductors exhibit intermediate Abrikosov vortices with Josephson cores, whose length  $l$  along GB is smaller than the London penetration depth, but larger than the coherence length. We found an exact solution for a periodic vortex structure moving along GB in a magnetic field  $H$  and calculated the flux flow resistivity  $R_F(H)$ , and the nonlinear voltage-current characteristics. The predicted  $R_F(H)$  dependence describes well our experimental data on  $7^\circ$  unirradiated and irradiated  $YBa_2Cu_3O_7$  bicrystals, from which the core size  $l(T)$ , and the intrinsic depairing density  $J_b(T)$  on nanoscales of few GB dislocations were measured for the first time. The observed temperature dependence of  $J_b(T) = J_{b0}(1 - T/T_c)^2$  indicates a significant order parameter suppression in current channels between GB dislocation cores.

PACS numbers: PACS numbers: **74.20.De**, **74.20.Hi**, **74.60.-w**

Mechanisms of current transport through grain boundaries (GB) in high-temperature superconductors (HTS) have attracted much attention, because a GB is a convenient tool to probe the pairing symmetry of HTS by varying the misorientation angle  $\vartheta$  between the neighboring crystallites [1, 2]. As  $\vartheta$  increases, the spacing between the GB dislocations decreases, becoming comparable to the coherence length  $\xi(T)$  at the angle  $\vartheta_0 \simeq 4 - 6^\circ$ . The exponential decrease of the GB critical current density  $J_b = J_0 \exp(-\vartheta/\vartheta_0)$  [2], makes GBs one of the principal factors limiting critical currents of HTS [3]. Atomic structure of GBs revealed by high-resolution electron microscopy have been used to determine local underdoped states of GB, defect-induced suppression of superconducting properties at the nanoscale and controlled increase of  $J_b$  by overdoping of GB [2, 4]. Much progress has been made in understanding the microscopic factors controlling  $J_b(\vartheta)$  at zero magnetic field, but the behavior of vortices on GBs is known to much lesser extent.

The extreme sensitivity of  $J_b(\vartheta)$  to the misorientation angle makes GB a unique tool to trace the fundamental transition between Abrikosov (A) and Josephson (J) vortices [5] in a magnetic field  $H$  above the lower critical field  $H_{c1}$ . For  $\vartheta \ll \vartheta_0$ , vortices on a GB are A vortices with normal cores pinned by GB dislocations [6]. For  $\vartheta > \vartheta_0$ , the maximum vortex current density circulating across the GB is limited to its *intrinsic*  $J_b(\vartheta)$ , much smaller than the bulk depairing current density  $J_d$ . Because vortex currents must cross the GB which can only sustain  $J_b \ll J_d$ , the normal core of an A vortex turns into a J core, whose length  $l \simeq \xi J_d/J_b$  along the GB is greater than  $\xi$ , but smaller than the London penetration

depth  $\lambda$ , if  $J_b > J_d/\kappa$ , where  $\kappa = \lambda/\xi \simeq 10^2$  [5]. As  $\vartheta$  increases, the core length  $l(\vartheta) \simeq \xi J_d/J_b(\vartheta)$  increases, so the GB vortices evolve from A vortices for  $\vartheta \ll \vartheta_0$  to mixed Abrikosov vortices with Josephson cores (AJ vortices) at  $J_d/\kappa < J_b(\vartheta) < J_d$ . The AJ vortices turn into J vortices at higher angles,  $\vartheta > \vartheta_J \simeq \vartheta_0 \ln(\kappa J_0/J_d)$ , for which  $l(\vartheta)$  exceeds  $\lambda$ . For  $\vartheta_0 = 5^\circ$ ,  $\kappa = 100$ , and  $J_0 = J_d$ , the AJ vortices determine the in-field behavior of GBs in the crucial region  $0 < \vartheta < \vartheta_J \simeq 23^\circ$  of the exponential drop of  $J_b(\vartheta)$  (in a film of thickness  $d \ll \lambda$ , the AJ region  $\vartheta < \vartheta_J \simeq \vartheta_0 \ln(\lambda^2/d\xi)$  broadens even further).

The AJ structures have two length scales: the core size  $l > \xi$  and the intervortex spacing  $a = (\phi_0/B)^{1/2}$ . The larger core of AJ vortices leads to their weaker pinning along a GB, which thus becomes a channel for motion of AJ vortices between pinned A vortices in the grains [5, 7] (Fig. 1). The percolative motion of AJ vortices along GBs gives rise to a linear region in the  $V - I$  characteristic of HTS polycrystals [6, 8, 9, 10, 11]. However no present experimental techniques can probe the cores of GB vortices, because the lack of the normal core makes AJ vortices "invisible" under STM, while neither the Lorentz microscopy nor magneto-optics have sufficient spatial resolution to distinguish A and AJ vortices. In this Letter we report a combined theoretical and experimental analysis which enabled us to prove the existence of AJ vortices in  $7^\circ$   $YBa_2Cu_3O_7$  bicrystals and extract the core size  $l(T)$ , and the intrinsic depairing current density  $J_b$  at the GB from transport measurements. The value  $J_b$  of a GB turns out to be much higher than its global critical current density  $J_{gb}$ , which is limited by self-field and pinning effects [7, 10, 11, 12, 13]. The

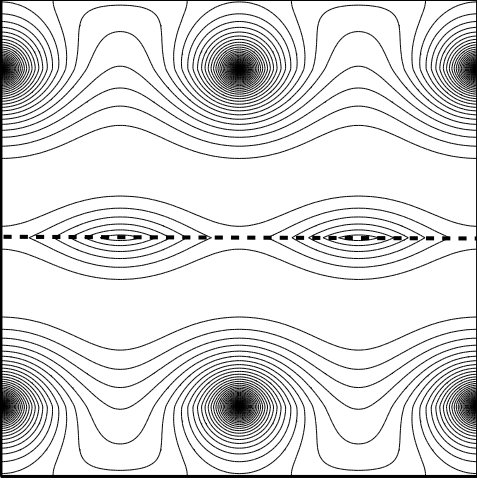


FIG. 1: Current streamlines around AJ vortices on a GB (dashed line) and the bulk A vortices in the grains, calculated from Eq. (5) for  $l = 0.2a$ .

field region in which only a single AJ vortex chain moves along GB while the bulk A vortices remain pinned, can be considerably expanded by irradiation, as shown below.

For  $H \gg H_{c1}$ , both  $l = \xi J_d / J_b$ , and  $a = (\phi_0 / B)^{1/2}$  are smaller than  $\lambda$ , thus the AJ vortices on low-angle GBs are described by a nonlocal equation for the phase difference  $\theta(x, t)$  in the overdamped limit [5, 7]:

$$\tau \dot{\theta} = \frac{l}{\pi} \int_{-\infty}^{\infty} \frac{\theta'(u) du}{u - x} - \sin \theta + \beta, \quad (1)$$

$$l = c\phi_0 / 16\pi^2 \lambda^2 J_b, \quad \tau = \phi_0 / 2\pi c R J_b, \quad (2)$$

where the overdot and the prime denote differentiation with respect to the time  $t$  and the coordinate  $x$  along GB,  $R$  is the quasiparticle resistance of GB per unit area,  $\phi_0$  is the flux quantum,  $c$  is the speed of light,  $\beta = J / J_b$ , and  $J(x)$  is the current density through GB induced by A vortices. Here  $\beta = \beta_0 + \delta\beta(x)$  is a sum of the constant transport current  $\beta_0$  and an oscillating component  $\delta\beta(x)$  due to the discreteness of the A vortex lattice. The term  $\delta\beta(x)$  gives rise to a critical current  $J_{gb}$  of the GB due to pinning of AJ vortices by A vortices in the grains [7, 14]. Eqs. (1) and (2) are independent of the pairing symmetry (which only affects  $J_b$ ) and are valid for both bulk samples and thin films in a perpendicular field.

We consider a rapidly moving AJ structure in the flux flow state,  $\beta \gg \beta_c$ , for which the pinning term  $\delta\beta(x) \ll 1$  can be neglected [14]. In this case Eq. (1) has the following *exact* solution that describes a stable periodic vortex structure moving with a constant velocity  $v$ :

$$\theta = \pi + \gamma + 2 \tan^{-1} [M \tan k(x - vt) / 2], \quad (3)$$

$$s^2 = [\sqrt{(1 - \beta_0^2 + h)^2 + 4\beta_0^2 h} - 1 - h + \beta_0^2] / 2h \quad (4)$$

Here  $s = v/v_0$ ,  $v_0 = l/\tau$ ,  $\tan \gamma = -s$ ,  $h = (kl)^2$ ,

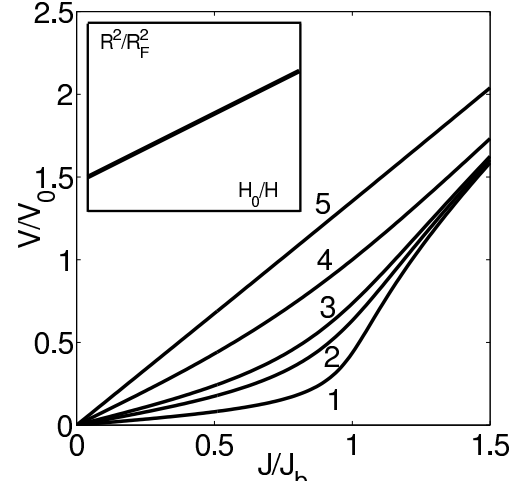


FIG. 2: The  $V - J$  curves calculated from Eq. (6) for different magnetic fields  $h = H/H_0$ : 0.01(1), 0.05(2), 0.1(3), 0.5(4), 10(5). Inset shows the field dependence of  $R_F(H)$ .

$M = [1 + 1/h(1 + s^2)]^{1/2} + [h(1 + s^2)]^{-1/2}$ ,  $k = 2\pi/a$ , and  $a$  is the period of the AJ structure. For  $a/l \rightarrow \infty$ , Eq. (3) describes a moving chain of single AJ vortices [5]. Generally,  $a(H)$  is different from the period of the A lattice, but for  $H \gg H_{c1}$ , the spacing  $a = (\phi_0/H)^{1/2}$  is fixed by the flux quantization condition. Eq. (3) corresponds to the following field distribution  $H(x, y)$  produced by AJ vortices in the region  $|y| < \lambda$ :

$$H = \frac{\phi_0}{2\pi\lambda^2} \text{Re} \ln \sin [x - vt + i(|y| + y_0)] \frac{k}{2}, \quad (5)$$

where  $\sinh ky_0 = \sqrt{h(1 + s^2)}$ . Eq. (5) satisfies the Maxwell equation  $\nabla^2 H = 0$  with the boundary condition  $H' = (4\pi/c)[J_b \sin \theta - \hbar v \theta' / 2eR - J]$  on GB, where  $\theta(x - vt)$  is given by Eq. (3). Fig. 1 shows the current streamlines calculated from Eq. (5). For  $y > 0$ , these streamlines coincide with those of a chain of moving fictitious A vortices displaced by  $y = -y_0$  away from GB.

The mean voltage  $V$  on a GB is determined by the Faraday law,  $V = \phi_0 v / ca$ , which yields

$$V = V_0 \left[ \sqrt{(1 - \beta_0^2 + h)^2 + 4\beta_0^2 h} - 1 - h + \beta_0^2 \right]^{1/2}, \quad (6)$$

where  $V_0 = R J_b / \sqrt{2}$ . The  $V - J$  curve shown in Fig. 2 is similar to that obtained by molecular dynamic simulations of incommensurate vortex channels [15]. In our case the nonlinearity of  $V(J)$  is due to the AJ core expansion as  $J$  increases [5]. For  $J \ll J_b$ , the  $V - J$  curve is linear,  $V = R_F J$ , where  $R_F = R \sqrt{h/(1 + h)}$  is the flux flow resistivity due to the viscous motion of AJ vortices. If  $H \gg H_{c1}$ , then  $h = (2\pi l/a)^2 = H/H_0$ , and

$$R_F = \frac{R \sqrt{H}}{\sqrt{H + H_0}}, \quad H_0 = \frac{\phi_0}{(2\pi l)^2} \quad (7)$$

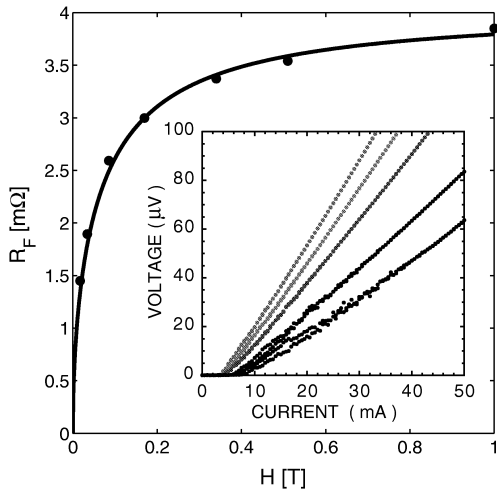


FIG. 3:  $R_F(H)$  data points extracted from the slopes of the  $V(J)$  curves at 77K and different  $H$  for unirradiated  $7^\circ$  bicrystal. The solid curves are described by Eq. (7) with  $R = 4.05m\Omega$  and  $H_0 = 0.14T$ . Inset shows  $V - J$  curves for 0.17kOe, 0.51kOe, 0.85kOe, 1.7kOe, and 3.4kOe (from bottom to top, respectively).

At  $H \ll H_0$ , Eq. (7) describes  $R_F(H)$  for AJ vortices, whose cores do not overlap. In this case  $R_F(H)$  is reminiscent of the 1D Bardeen-Stephen formula,  $R_{BS} \simeq R\sqrt{H/H_{c2}}$ , except that in Eq. (7) the core structure is taken into account exactly. For  $H > H_0 \simeq (J_b/J_d)^2 H_{c2} \ll H_{c2}$ , the AJ cores overlap, and Eq. (7) describes a crossover to a field-independent quasiparticle resistance of GB. This regime has no analogs for A vortices, whose normal cores overlap only at  $H_{c2}$ . The simplicity of Eq. (7) enabled us to extract intrinsic GB properties from the measurements of  $R_F(H)$ .

We observed the AJ vortex behavior on  $7^\circ YBa_2Cu_3O_7$  bicrystals with a sharp resistive transition  $\Delta T < 0.4K$  at  $T_c = 91K$ . Thin films of thickness 250 nm were grown on [001]-oriented  $SrTiO_3$  bicrystals by pulsed laser deposition at 210 mTorr oxygen pressure and 810°C, and then annealed in oxygen at 830 Torr and 520°C for 30 min. One  $7^\circ$  bicrystal was irradiated with 1GeV Pb ions at a fluence corresponding to 1T. Bridges 25  $\mu m$  wide were patterned by Ar ion beam etching on a cooled sample mount to produce a four-point measurement geometry, as described in Ref. [9]. The voltage probes were 100 $\mu m$  apart, on either sides of the GB.  $V - I$  curves were measured in a gas-flow cryostat in fields  $0 < H < 10$  T. Both samples are in the transition region of  $\vartheta$  between strongly coupled bicrystals that behave in a manner similar to the single-crystal grains, and weakly coupled bicrystals that demonstrate the Josephson effect[13]. The intragrain  $J_c$  values at 77 K were  $0.1MA/cm^2$  and  $0.27MA/cm^2$  for the unirradiated and irradiated samples, respectively.

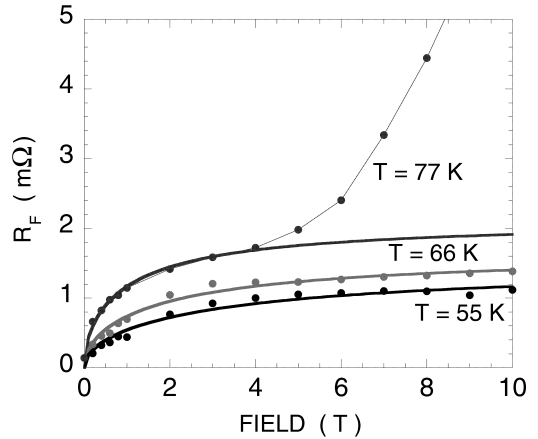


FIG. 4:  $R_F(H)$  extracted from the slopes of  $V(J)$  for different  $T$  and  $H$  for the irradiated  $7^\circ$  bicrystal. The  $V - J$  curves have the extended linear regions similar to those for the unirradiated sample shown in Fig. 3. The solid curves are described by Eq. (7) with two fit parameters  $R$  and  $H_0$ .

Fig. 3 shows V-I characteristics for the unirradiated sample at 77K and different magnetic fields. The V-I curves exhibit linear flux flow portions in a wide range of  $I$  above the depinning critical current  $I_{gb}(H)$  which decreases with  $H$  [13]. In this work we focus on the flux flow region  $I \gg I_{gb}$ , where the dynamic resistance  $R_F(H) = dV/dI$  increases as  $\sqrt{H}$  at low  $H$ , but levels off at higher  $H$ . We found that Eq. (7) describes the observed  $R_F(H)$  very well, thus the vortex cores on this GB overlap at  $H \sim H_0$ , well below  $H_{c2}$ . Because the GB can sustain a finite supercurrent  $I_{gb}$  even for  $H > H_0$ , the GB vortices lack normal cores. The good fit in Fig. 3 enabled us to extract  $R = 4.05m\Omega$  and  $H_0 = 0.14T \ll H_{c2}$  by plotting  $1/R_F^2(H)$  versus  $1/H$ , as shown in Fig. 2. Using Eq. (7), we obtain that  $l = (\phi_0/H_0)^{1/2}/2\pi = 190\text{\AA}$  at 77K, thus vortices on this  $7^\circ$  GB are indeed AJ vortices with phase cores much greater than  $\xi(T) = \xi_0/\sqrt{1-T/T_c} \simeq 40\text{\AA}$  but smaller than  $\lambda = \lambda_0/\sqrt{1-T/T_c} \simeq 4000\text{\AA}$  for  $\xi_0 \simeq 15\text{\AA}$ ,  $\lambda_0 \simeq 1500\text{\AA}$ , and  $T_c = 91K$ .

$R_F(H)$  data for the irradiated bicrystal at different  $T$  are shown in Fig. 4. The good agreement between Eq. (7) and the observed  $R_F(H)$  enabled us to extract the temperature dependences of  $H_0$  and  $R$  shown in Fig. 5. While  $R(T)$  varies only weakly, the field  $H_0(T)$  exhibits a parabolic dependence,  $H_0(T) = H_0(0)(1-T/T_c)^2$  with  $H_0(0) \approx 42T$ . As follows from Eq. (7), the fact that  $H_0(T) \propto (T_c - T)^2$  implies  $l(T) \propto (T_c - T)^{-1}$ , which, in turn, indicates the SNS behavior of  $J_b(T) \propto (T_c - T)^2$ , if  $\lambda(T) \propto (T_c - T)^{-1/2}$  in Eq. (2). From the data in Fig. 5, we can also obtain the absolute value of the intrinsic depairing current density  $J_b$  averaged over the

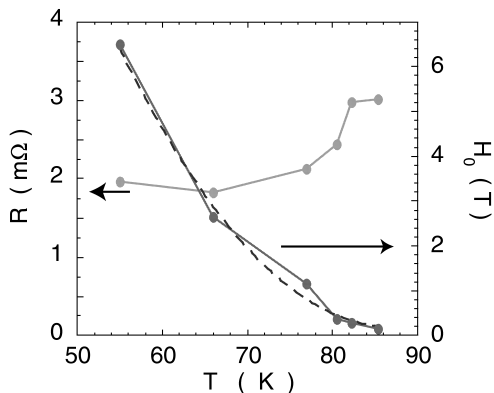


FIG. 5:  $R(T)$  and  $H_0(T)$  extracted from the fit procedure represented in Fig. 4. The dashed line shows  $H_0 = 42(1 - T/T_c)^2$  [Tesla].

Josephson core length  $l$ . To do so, we write Eq. (7) in the form  $J_b = (3J_d/4)\sqrt{6\pi H_0/H_{c2}}$ , which express  $J_b$  in terms of the measured parameters  $H_0$ ,  $H_{c2} = \phi_0/2\pi\xi^2$ , and  $J_d = c\phi_0/12\sqrt{3}\pi^2\lambda^2\xi$ . For  $H_{c2}(T) = H'_{c2}(T_c - T)$ , this yields  $J_b \simeq (3J_d/4)[6\pi H_0(0)/T_c H'_{c2}]^{1/2}(1 - T/T_c)^{1/2}$ , whence  $J_b(85K) \simeq 0.3J_d(85K)$  for  $H_0(0) = 42T$ , and  $H'_{c2} = 2T/K$ . Likewise we get  $J_b(77K) \simeq 0.23J_d(77K)$  for the unirradiated sample, ( $H_0(77K) = 0.14T$ ). Therefore, our data indicate a significant suppression of the order parameter, even on the low-angle  $7^\circ$  GB, in agreement with the model of Ref. [16].

For the observed  $H_0(T)$ , the AJ core length  $l(T) = (\phi_0/H_0(T))^{1/2}/2\pi \simeq 11(1 - T/T_c)^{-1}[\text{\AA}]$ , exceeds the bulk coherence length  $\xi(T) = \xi_0/\sqrt{1 - T/T_c}$  at  $T_c - T \ll T_c$ , but remains smaller than  $\lambda(T)$ , except very close to  $T_c$ . For instance, we obtain  $l(80K) \simeq 91\text{\AA}$ , while  $\xi(80K) \simeq 43\text{\AA}$ , and  $\lambda(80K) = 4300\text{\AA}$ . The length  $l(T)$  also exceeds the GB dislocation spacing  $\simeq 32\text{\AA}$ , thus the moving AJ cores probe GB properties averaged over few current channels between dislocations. The core length  $l(\vartheta) \simeq \xi J_d/J_b(\vartheta)$  increases as  $\vartheta$  increases, becoming larger than  $\lambda$ , if  $\vartheta > \vartheta_0 \ln \kappa$ , in which case AJ vortices turn into J vortices. Since the ratio  $J_b/J_d$  decreases as  $T$  increases, higher-angle GBs can exhibit AJ vortices at low  $T$  and J vortices at  $T \approx T_c$ , while lower angle GBs have A vortices at low  $T$  and AJ vortices at  $T \approx T_c$ .

The depinning current density  $J_{gb}$  seen in Fig. 3 is due to interactions of AJ vortices with microstructural inhomogeneities along GB and pinned A vortices in the grains[5]. Another essential mechanism occurs if the periods of AJ and A vortices do not coincide, resulting in misfit dislocations in the AJ chain[15]. These vortex dislocations can strongly limit  $J_{gb}$  because their intrinsic pinning by the A vortex lattice is exponentially weak[15]. For  $H \gg H_{c1}$ , when the AJ and A periods are close, the pinning of a few misfit dislocations in the AJ chain may be thus dominated by macroscopic  $T_c$  and  $J_b(x)$  varia-

tions along GB caused by facet structures, strain fields, local nonstoichiometry, etc. [17]. In this Letter we focus on the flux flow state  $J \gg J_{gb}$ , where pinning weakly affects  $R_F$ . In this case measurements of  $R_F(H)$  reveal the essential physics of GB vortices whose moving AJ cores probe intrinsic properties of GBs at the nanoscale, regardless of particular pinning mechanisms which are essential at  $J \approx J_{gb}$ . Because the observed  $V - J$  curves are nearly linear above  $J_{gb}(77K, 1T) \sim 10^4 - 10^5 A/cm^2 \ll J_b \simeq (0.2 - 0.3)J_d \sim 1 - 10 MA/cm^2$ , the pinning region  $J \sim J_{gb}$  is much smaller than the scale of Fig. 2. Thus, the nonlinearity of  $V(J)$  due to the AJ core expansion does not affect  $R_F$  measured at  $J < 3J_{gb}$  so Eq. (7) can be used to fit the data. A similar approach was used to measure the flux flow resistivity of pinned A vortices driven by strong current pulses well above  $J_c$ [18].

The case when only a single AJ vortex row moves along the GB, while the intragrain A vortices remain pinned corresponds to low fields,  $H < H_1$ . For  $H > H_1$ , the AJ vortices drag neighboring A vortices in the flux flow channel along GB [7]. The field  $H_1$  can be estimated from the condition that the pinning force  $f = \phi_0\Delta H/2a(H)$  of AJ vortices due to their magnetic interaction with A vortices equals the bulk pinning force  $\phi_0 J_c/c$ , where  $\Delta H = \phi_0 e^{-2\pi u/a}/\pi\lambda^2$  is the amplitude of the oscillating part of the local field  $H(x) \approx B + \Delta H \cos(2\pi x/a)$  produced by A vortices along GB, and  $u$  is the spacing of the first A vortex row from GB[14]. Therefore,

$$H_1 \simeq 4\phi_0 J_c^2(H_1)/c^2 \Delta H^2 \quad (8)$$

Transitions from a single to a multiple row vortex motion [9, 11] result in a sharp upturn of the  $R_F(B, 77K)$  curve at  $H_1 \simeq 4T$  in Fig. 4. Here  $H_1$  for our unirradiated sample ( $J_c = 0.1 MA/cm^2$ ) is 7.3 times smaller than  $H_1$  for the irradiated one ( $J_c = 0.27 MA/cm^2$ ). For  $\lambda(77K) \simeq 4000\text{\AA}$ , and  $H_1 = 4T$ , Eq. (8) yields  $u = \ln(c^2 H_1 \phi_0 / 4\pi^2 \lambda^4 J_c^2) / 4\pi = 0.92a$ .

In conclusion, vortices on low-angle grain boundaries in HTS are mixed Abrikosov-Josephson vortices. Exact solutions for a moving AJ vortex structure, the nonlinear  $V - J$  characteristic and the flux flow resistivity  $R_F(B)$  were obtained. From the measurements of  $R_F(B)$  on a  $7^\circ$  YBCO bicrystal, we extracted the length of the AJ core and the intrinsic depairing current density  $J_b$  on GB. The analysis proposed in this work can be used for systematic studies of the effect of overdoping [4] on the local suppression of the order parameter and current transport through nanoscale channels between GB dislocations.

This work was supported by the NSF MRSEC (DMR 9214707), AFOSR MURI (F49620-01-1-0464), and by Italian INFN-PRA JT3D.

- 
- [1] C.C. Tsuei and J.R. Kirtley, Rev. Mod. Phys. **72**, 969 (2000).
- [2] H. Hilgenkamp and J. Mannhart, Rev. Mod. Phys. **74**, (2002).
- [3] D.C. Larbalestier, A. Gurevich, D.M. Feldmann, and A.A. Polyanskii, Nature **413**, 368 (2001).
- [4] S.E. Russek *et al.*, Appl. Phys. Lett. **57**, 1155 (1990); A. Schmehl *et al.*, Europhys. Lett. **47**, 110 (1999); G. Hammerl *et al.*, Nature **407**, 162 (2000); K. Guth *et al.*, Phys. Rev. B **64**, R140508 (2001).
- [5] A. Gurevich, Phys. Rev. B **46**, R3187 (1992); **48**, 12857 (1993); Physica C**243**, 191 (1995).
- [6] A. Diaz *et al.*, Phys. Rev. Lett. **80**, 3855 (1998); Phys. Rev. B **58**, R2960 (1998).
- [7] A. Gurevich and L.D. Cooley, Phys. Rev. B **50**, 13363 (1994).
- [8] D.T. Verebelyi *et al.*, Appl. Phys. Lett. **76**, 1755 (2000); **78**, 2031 (2001).
- [9] G.A. Daniels, A. Gurevich, and D.C. Larbalestier, Appl. Phys. Lett. **77**, 3251 (2000).
- [10] D. Kim *et al.*, Phys. Rev. B **62**, 12505 (2000); J. Albrecht *et al.*, Phys. Rev. B **61**, 12433 (2000).
- [11] M.J. Hogg *et al.*, Appl. Phys. Lett. **78**, 1433 (2001).
- [12] K.E. Gray *et al.*, Phys. Rev. B **58**, 9543 (1998).
- [13] R.D. Redwing *et al.*, Appl. Phys. Lett. **75**, 3171 (1999).
- [14] The pinning force of AJ vortices is the maximum gradient of the magnetic energy  $f(x) = -\phi_0 \partial_x H(x)/4\pi$ , where  $H(x) \approx B + \Delta H \cos(2\pi x/a)$  is the local field of the A vortex lattice along GB,  $\Delta H = (\phi_0/\pi\lambda^2) \exp(-2\pi u/a)$  at  $H \gg H_{c1}$  and  $u \approx a$ . Thus,  $f_m = \phi_0 \Delta H/2a$ ,  $\delta\beta(x) = c\partial_x H(x)/4\pi J_b = \beta_1 \cos(2\pi x/a)$ , and  $\beta_1 = c\Delta H/2aJ_b = 4(H/H_0)^{1/2} \exp(-2\pi u/a)$ . This yields the pinning correction to the resistivity,  $R(J) - R_F \sim -R_F J_{gb}^2/J^2$  for  $J \gg J_{gb}$ . Here  $\beta_1 \ll 1$  in a wide field range  $H < 2 \times 10^4 H_0$ , where GB is transparent to local currents  $J_v = c\partial_x H(x)/4\pi < J_b$  of A vortices.
- [15] R. Besseling, R. Niggerbrugge, and P.H. Kes, Phys. Rev. Lett. **82** 3144 (1999).
- [16] A. Gurevich and E.A. Pashitskii, Phys. Rev. B **57**, 13878 (1998).
- [17] X.Y. Cai *et al.*, Phys. Rev. B **57**, 10951 (1998).
- [18] M.N. Kunchur *et al.*, Phys. Rev. Lett. **84**, 5204 (2000).